Journal of Asian Earth Sciences 36 (2009) 38–46

Contents lists available at ScienceDirect

Journal of Asian Earth Sciences

journal homepage: www.elsevier.com/locate/jaes

Analytical and numerical simulation of tsunami mitigation by mangroves in Penang, Malaysia

Su Yean Teh [a], Hock Lye Koh [a,*], Philip Li–Fan Liu [b], Ahmad Izani Md. Ismail [a], Hooi Ling Lee [c]

[a] School of Mathematical Sciences, Universiti Sains Malaysia, 11800 Gelugor, Penang, Malaysia
[b] School of Civil and Environmental Engineering, Cornell University, USA
[c] Technip GeoProduction (M) Sdn Bhd, Kuala Lumpur, Malaysia

ARTICLE INFO

Article history:
Received 28 April 2008
Received in revised form 28 September 2008
Accepted 30 September 2008

Keywords:
Andaman tsunami
Runup simulation
Mangrove forest

ABSTRACT

The Andaman tsunami that occurred on 26 December 2004 killed about a quarter million people worldwide, of which 52 deaths happened in Penang, Malaysia. Mangrove forests fringing the shallow coastal seas of Penang Island and northwest of Peninsular Malaysia have been credited to have played a role in mitigating the tsunami waves. It is therefore relevant to assess the role of mangroves in tsunami mitigation by analytical model and numerical simulations. The role of mangrove forest in reducing tsunami wave energy, heights and velocities are simulated by the incorporation of the Morison Equation to represent friction provided by the mangrove forest for the coasts of Penang. Wave heights and velocities can be reduced in the presence of mangrove. However the degree of reduction varies significantly depending on several factors such as wave period and wavelength as well as mangrove characteristics including forest widths and density. For a wave of 10 km wavelength, with wave height and velocity of 1.0 m and 1.0 m/s, respectively at the shore without a mangrove forest, then a mangrove forest of 500 m width may provide a reduction ratio for wave height and wave velocity of about 0.55 and 0.50, respectively.

1. Introduction

The 26 December 2004 Andaman tsunami resulted in the death of about a quarter million people worldwide. Simulation of the generation, propagation and runup of tsunami waves has become a priority research among scientists in the affected coastal regions including Malaysia. Concerted effects have been devoted to rehabilitate mangrove forests in Malaysia with the hope to provide some mitigation in the event of future tsunamis or storm surges. This provides the motivation to simulate the potential mitigation effects of mangroves in reducing the adverse impacts of tsunami along the coastal regions covered by mangrove. It has been reported that tsunami wave energy, heights and velocities may be significantly reduced as the wave propagates through mangrove forests (Harada and Kawata, 2004; Hiraishi and Harada, 2003; Harada and Imamura, 2000). However, some controversy regarding the mitigation effects of wave impacts by mangrove forest has been reported over the literature (Baird, 2006; Chatenoux and Peduzzi, 2006). Shuto (1987) has noted that if the wave heights exceed 4 m, the mangrove trees may be uprooted; creating debris that might cause secondary harm. The effects played by mangroves depend on several factors such as forest width and density as well as wavelength and period. Hence we will investigate the role of mangrove in reducing the wave heights and velocities subject to several factors including wavelength and period, mangrove forest width and other mangrove forest characteristics.

In a related study (Koh et al., 2008a), the propagation of the Andaman tsunami from the tsunami source to the offshore regions in Malaysia up to the depth of 50 m has been simulated by an in-house model TUNA-M2, with a grid size of 1000 m. In this paper, we simulate tsunami wave runup through mangrove forests fringing the shallow coastal areas in Penang by the non-linear shallow water equation (NSWE). The wave heights and velocities at 50 m depth offshore simulated by the propagation model TUNA-M2 (Koh et al., 2008b; Koh, 2004) are used as input to simulate wave runup through mangrove along shallow coasts by the runup model TUNA-RP (Teh et al., 2008). Simulations of tsunami wave through mangrove forests are performed by the incorporation of the Morison Equation to mimic friction into the momentum equation (Harada and Imamura, 2005). Basically, the Morison equation provides a friction term to reduce wave energy. Grid sizes between 20 m to 40 m are used, as these grids are able to provide general information about the wave height and velocity in the mangroves.

2. Numerical schemes for TUNA-RP

The numerical scheme for TUNA-M2 is described in detail in Koh et al. (2008a) and hence omitted here. To simulate wave runup

* Corresponding author. Tel.: +60 4 6533657; fax: +60 4 6570910.
E-mail address: hlkoh@cs.usm.my (H.L. Koh).

1367-9120/$ - see front matter © 2008 Elsevier Ltd. All rights reserved.
doi:10.1016/j.jseaes.2008.09.007

along the shallow seas, the NSWE given by Eqs. (1) and (2) are used.

$$\frac{\partial \eta}{\partial t} + \frac{\partial (u(\eta + h))}{\partial x} = 0 \tag{1}$$

$$\frac{\partial u}{\partial t} + u\frac{\partial u}{\partial x} + g\frac{\partial \eta}{\partial x} = 0 \tag{2}$$

Here t (s) is time, x (m) is distance. Further η (m) is the wave height above mean sea level, u (m/s) the horizontal velocity in the x-direction, h (m) the still water depth and g (m/s^2) the gravitational acceleration. Henceforth the same notations will be used throughout without further definition, with the unit of a notation given within a pair of brackets.

Explicit finite difference method is used to solve the NSWE. Two numerical schemes are tested for the purpose of evaluating their accuracy and numerical stability. The first scheme is the forward in time central in space (FTCS) scheme (Marchuk and Anisimov, 2001), hereafter named CRP. The second scheme is the staggered scheme (Koh, 2004) named SRP. The finite difference approximations for the NSWE by means of the FTCS (CRP) and the staggered scheme (SRP) are shown in Eqs. (3) and (4), respectively. Subscript i refers to spatial step, while superscript n refers to time step. The central scheme CRP involves only full integer nodes, while the staggered scheme SRP involves also half-integer spatial steps (i-0.5) and half-integer time steps (n-0.5), in addition to full integer nodes. Spatial grid is denoted by Δx (m) and time step by Δt (s).

$$\begin{aligned}
&\frac{u_i^n - u_i^{n-1}}{\Delta t} + u_i^{n-1}\frac{(u_{i+1}^{n-1} - u_{i-1}^{n-1})}{2\Delta x} + g\frac{(\eta_{i+1}^{n-1} - \eta_{i-1}^{n-1})}{2\Delta x} = 0\\
&\frac{\eta_i^n - \eta_i^{n-1}}{\Delta t} + (h_i + \eta_i^{n-1})\frac{u_{i+1}^n - u_{i-1}^n}{2\Delta x}\\
&\quad + u_i^n\frac{h_{i+1} + \eta_{i+1}^{n-1} - h_{i-1} - \eta_{i-1}^{n-1}}{2\Delta x} = 0
\end{aligned} \tag{3}$$

$$\begin{aligned}
&\frac{\eta_i^n - \eta_i^{n-1}}{\Delta t} + (h_i + \eta_i^{n-1})\frac{u_{i+0.5}^{n-0.5} - u_{i-0.5}^{n-0.5}}{\Delta x}\\
&\quad + u_{i+0.5}^{n-0.5}\frac{h_{i+1} + \eta_{i+1}^{n-1} - h_i - \eta_i^{n-1}}{\Delta x} = 0\\
&\frac{u_{i+0.5}^{n+0.5} - u_{i+0.5}^{n-0.5}}{\Delta t} + u_{i+0.5}^{n-0.5}\frac{(u_{i+0.5}^{n-0.5} - u_{i-0.5}^{n-0.5})}{\Delta x} + g\frac{(\eta_{i+1}^n - \eta_i^n)}{\Delta x} = 0
\end{aligned} \tag{4}$$

Fig. 1 shows the locations of the elevation η and velocity u points in the CRP scheme, where both η and u occupy the same full integer locations or nodes. Fig. 2 displays the locations of η and u points in the SRP staggered scheme, in which elevation η is located at the full integer nodes for both x and t, while velocity u is located at half-integer nodes for both x and t. The location of η point is represented by a circle, while the location of u point is represented by a cross for both Figs. 1 and 2. Essentially η and u are evaluated at the full integer nodes η_i^n and u_i^n in CRP. However in SRP η is evaluated at full integer nodes such as η_i^n, while u is evaluated at half-integer nodes such as $u_{i+0.5}^{n-0.5}$. This implies that only η needs to be prescribed on the boundary (right hand side of Fig. 2) with full integer nodes but not u with half-integer nodes for SRP. Intuitively this translates to the consequence that one condition less is required on the boundary for SRP. This would induce less computational errors when inaccurate approximation of radiation boundary conditions (RBC) is implemented. In short, SRP is intuitively expected to perform better than CRP, particularly when long computations are performed for distant tsunami where RBC cannot be perfectly prescribed to allow the wave to propagate out of the computational domain with minimal or no reflection. Cumulative errors over long cycles of interactions would soon overwhelm the solutions. To provide complete mathematical verification of this intuitive observation is beyond the scope of this paper.

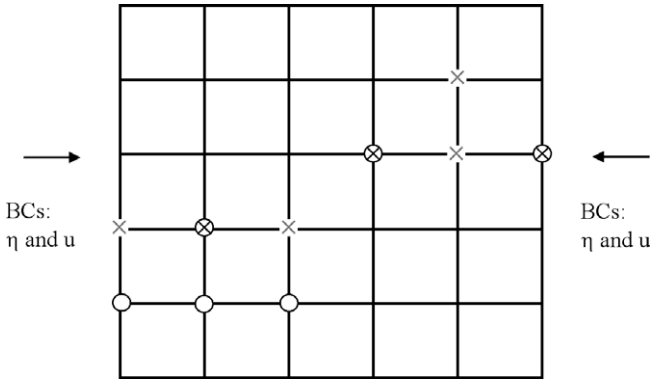

Fig. 1. FCTS scheme (CRP), with two boundary conditions imposed.

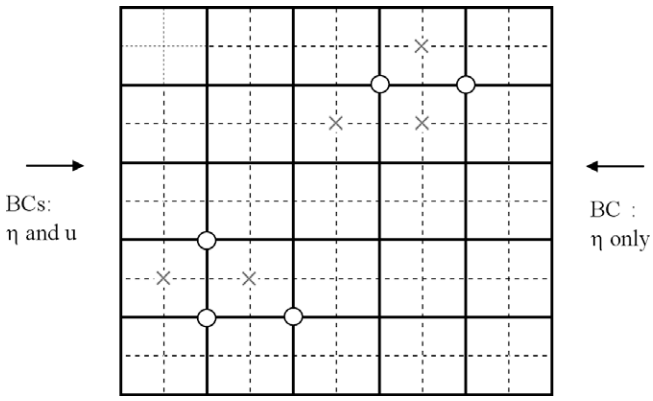

Fig. 2. Staggered scheme (SRP), with one boundary condition imposed.

With this observation in mind we will demonstrate in Section 3.2 that the SRP scheme is indeed more accurate and more stable than the CRP scheme, particularly over long cycle of iterations. The main season for this accuracy lies in the manner in which the boundary conditions are implemented in SRP as discussed above.

3. Implementation of boundary conditions

3.1. Radiation open boundary

An appropriate RBC would technically allow waves to pass through the open boundary freely without reflections. Three methods of applying the radiation boundary will be tested for their efficiency and accuracy. The first method is a commonly used RBC that equates wave at the boundary node to the wave at the upstream node at the previous time step. This is equivalent to a 1-node interpolation and will be referred to as RBC1. A second scheme named RBC2 is one based upon a 2-point interpolation, where the wave at the previous time step at two upstream locations are used to estimate wave heights at the present time step by simple interpolation. The third scheme RBC3 proposed is based upon a 4-point interpolation, where the waves at the previous time step at four upstream locations are used to interpolate the wave heights at the present time step by the method of characteristics. The method of characteristics essentially allows the wave profile at the previous time step to propagate forward freely. It will be shown in Section 3.3 that RBC3 would produce the best simulation results. Hence RBC3 will be used in the next section for the purpose of comparing the performance of CRP and SRP.

3.2. Comparison between CRP and SRP

Next, we will compare the performance of the CRP and SRP schemes using 4-point interpolation RBC3 for both schemes. For this purpose, we use a simple tide with a period of 12 h, amplitude of 1 m and mean depth h of 9.81 m as shown in Eq. (5). The analytical solution is

$$\eta = \sin(\sigma t - kx), \quad u = \sqrt{\frac{g}{h}}\sin(\sigma t - kx), \quad k = \sigma/\sqrt{gh} \tag{5}$$

Here $\sigma = 1.4544 \times 10^{-4}\ s^{-1}$ is the frequency of the wave corresponding to the period of 12 h and $k = 1.4826 \times 10^{-5}\ m^{-1}$ is the wave number. The remaining notations are defined in Section 2. To accommodate a complete sinusoidal wave, the domain is chosen to be $2\pi/k = 432$ km long, with $\Delta x = 1000$ m and $\Delta t = 60$ s. For convenience, the depth and the gravity are chosen so that $u = \eta$ in the numerical values. The wave is allowed to enter the test domain from the left boundary (upstream) by prescribing $\eta = \sin(\sigma t - kx)$, $u = \sqrt{\frac{g}{h}}$. The wave is allowed to leave the test domain freely through the right (downstream) boundary. This is done numerically by prescribing the RBC using the 4-point interpolation RBC3, as discussed above, at the right hand side (downstream) of the test domain. The simulated results using CRP are shown in Fig. 3 at several time intervals. After 12 h (Fig. 3a), the simulated η and u agree with the analytical solution. However, the numerical error grows gradually (Fig. 3b) until the simulated results bear no resemblance to the analytical solution at 48 h (Fig. 3c). On the other hand, the simulated results by SRP using RBC3 agree closely with the analytical solution for the entire duration of 48 h (Fig. 3d, e and f). Various numerical testing indicates that SRP is superior to CRP, as SRP requires one less boundary condition on the downstream boundary than CRP (Figs. 1 and 2) and hence induces less errors. Hence, SRP will be incorporated with RBC3 into TUNA-RP in this study. Indeed CRP often demonstrates numerical instability while SRP remains stable for the same numerical runs.

3.3. Comparison among RBCs

We will use the staggered numerical scheme in TUNA-RP to test the performance of three RBCs mentioned earlier. The sinusoidal wave is allowed to enter the test domain from the left boundary (upstream) by imposing η and u in Eq. (5) at this point. The wave is allowed to pass out of the downstream open boundary at the right hand side. Numerically, the three RBCs described above are implemented to represent these downstream open boundary conditions. The simulated results are shown in Fig. 4 after 60 h of wave propagation. It is clear that the 4-point interpolation scheme implemented by RBC3 (Fig. 4b) performs best as compared to the

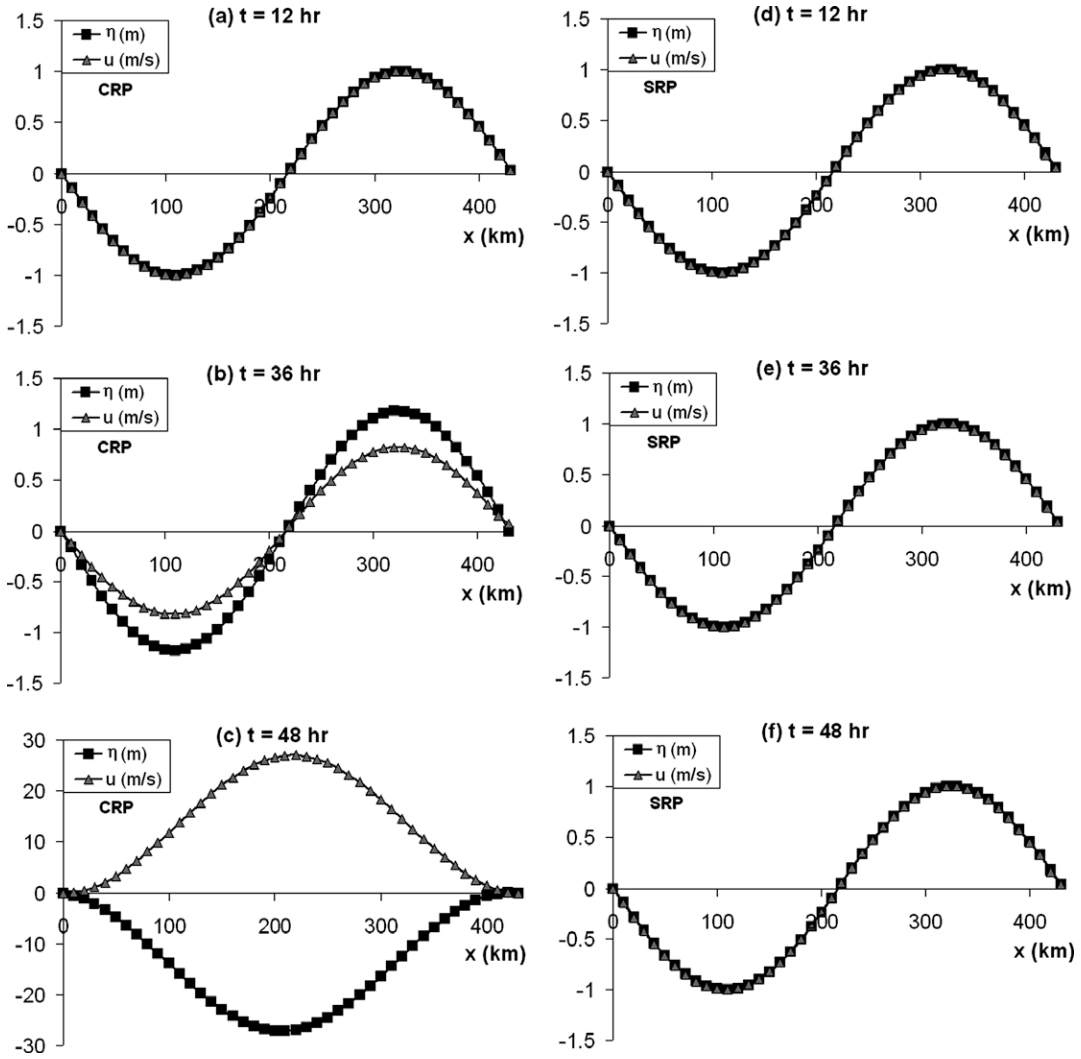

Fig. 3. CRP (left) and SRP (right) simulated η and u for a semi-diurnal tide at 12, 36 and 48 h.

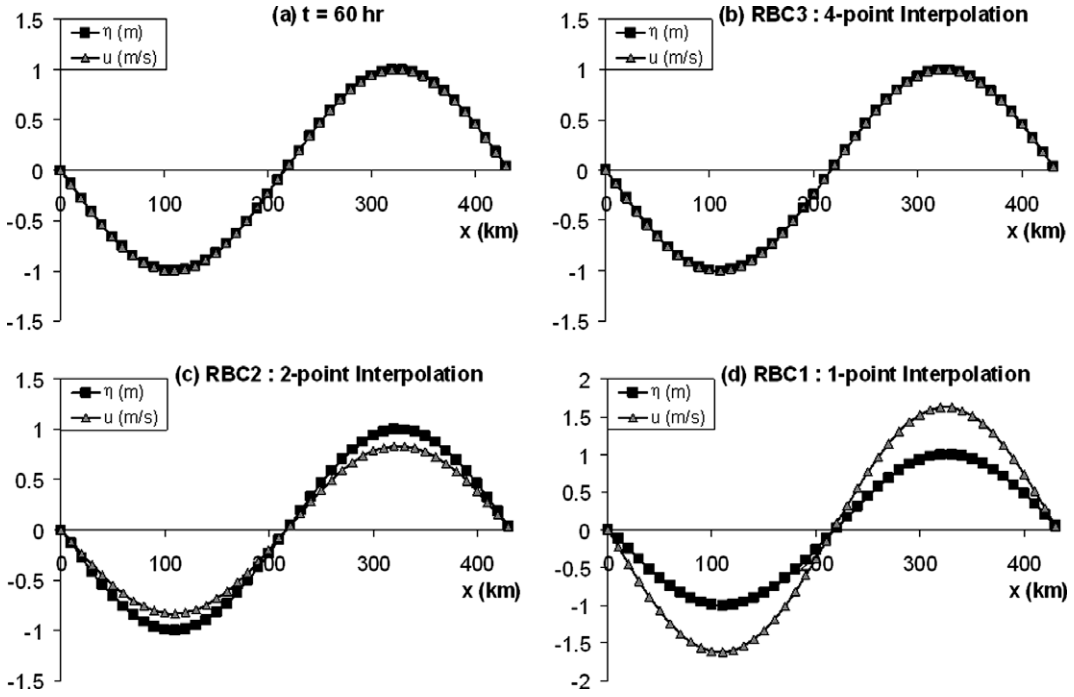

Fig. 4. (a) Analytical solution, (b) TUNA-RP simulated η and u by RBC3, (c) RBC2 and (d) RBC1.

other two. Boundary conditions represented by RBC1 produce significant errors (Fig. 4d), hence is not used in our study.

4. Morison equation

To represent friction created by mangrove, Harada and Imamura (2005) incorporated the Morison's Equation into the momentum Eq. (6) to assess the impact of coastal mangrove forest on the hydrodynamics of tsunami.

$$\frac{\partial M}{\partial t}+\frac{\partial}{\partial x}\left(\frac{M^2}{D}\right)+gD\frac{\partial \eta}{\partial x}+\frac{gn^2M|M|}{D^{7/3}}+\frac{C_d}{2}A_0\frac{M|M|}{D^2}+C_m\frac{V_0}{V}\frac{\partial M}{\partial t}=0 \quad (6)$$

In the above, M = flow flux (m^2/s), $D=(\eta+h)$ = total water depth (m), h = still water depth (m), n = Manning coefficient ($sm^{-1/3}$) and g = gravitational acceleration (m/s^2). Friction terms are parameterized by the two coefficients C_d = drag coefficient (dimensionless) and C_m = inertia coefficient (dimensionless). Finally the characteristics of mangrove forest are represented by three parameters, namely A_0 (m^2 per 100 m^2) = projected area of trees under water surface (per 100 m^2), V_0 (m^3) = volume of trees under water surface within a chosen control volume V (m^3). Eq. (6) is discretized by the finite difference method, the details of which are available in Teh (2008) hence omitted here.

To calculate the drag coefficient C_d and inertia coefficient C_m, Harada and Imamura (2003) proposed the following Eq. (7), based upon data collected on coastal pine trees forest in Japan.

$$C_d=8.4\frac{V_0}{V}+0.66 \quad \left(0.01\leqslant\frac{V_0}{V}\leqslant 0.07\right)$$
$$C_m=1.7 \quad (7)$$

Based upon the range of V_0/V given in Eq. (7) for coastal pine forests in Japan, if we choose the values of 0.01 and 0.07 for V_0/V, then C_d is given by 0.744 and 1.248, respectively, which are in the lower end of the range of values of between 0.4–10 for C_d, derived by Mazda et al. (1997) for mangrove. This arises probably because pine forest has relatively smaller value of V_0/V as compared to mangrove. Values of A_0 and V_0/V for Penang mangrove forests are computed internally within TUNA-RP based upon mangrove forest characteristics monitored during the field surveys conducted on the Penang site as described below.

The modeled mangrove tree is envisaged as a structure consisting of three parts: root system, stem (trunk) and leaf (canopy), formed by cylinders of different diameters and heights. Fig. 5 shows the model representation of *Avicennia officinalis*, a species of mangrove with pencil roots commonly found in Penang study site. The values of projected area of trees under water surface (A_0 per 100 m^2) and volume of trees under water surface (V_0 m^3) within a control volume V (m^3) are calculated by the formulas indicated below (Hiraishi and Harada, 2003), where the notations are defined in Fig. 5 for clarity. The subcripts R, T and L refer to root, trunk and leaf, respectively. The notations A (m^2), H (m), D (m), V (m^3) and P (dimensionless fraction) denote area, height, diameter, volume and leaf porosity, respectively. Finally N_R and N_T are the number of roots per tree and number of trees per 100 m^2. Each of these parameters must be measured or estimated. Note that only those parts of the trees that are submerged in water contribute to the drag and inertia terms.

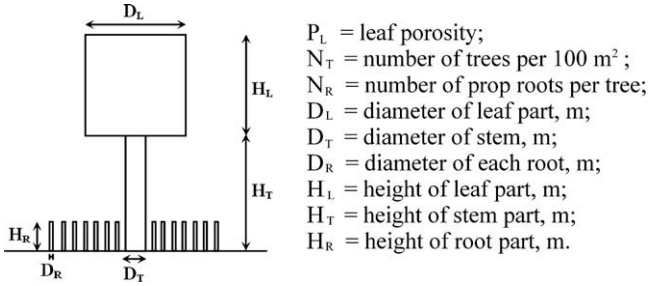

Fig. 5. Modeled mangrove tree.

$$A_0 = A_R + A_T + A_L;$$
$$A_R = H_R\left(D_R\frac{N_R N_T}{100}\right),\ A_T = H_T\left(D_T\frac{N_T}{100}\right)$$
$$\text{and } A_L = P_L \times H_L\left(D_L\frac{N_T}{100}\right).$$

$$V_0 = V_R + V_T + V_L;$$
$$V_R = H_R\left(\pi\frac{D_R^2}{4}N_R N_T\right),\ V_T = H_T\left(\pi\frac{D_T^2}{4}N_T\right)$$
$$\text{and } V_L = P_L \times H_L\left(\pi\frac{D_L^2}{4}N_T\right).$$

The values of A_0 and V_0/V are computed internally in TUNA-RP based upon input data measured in the mangrove forest in Penang regarding the mangrove physical characteristics discussed above. These computed friction parameters are used in the Morison Equation to simulate the impact of mangroves on the hydrodynamics of tsunami over the mangrove forest in Penang. For Penang, a range of V_0/V values is estimated to fall between 0.04 and 0.16, resulting in values of C_d between 0.7 and 2.0, which is in the lower range of C_d between 0.4–10 reported by Mazda et al. (1997). Mazda et al. (1995) investigated the role of drag resistance on the tidal flows of mangrove swamps by means of numerical simulations.

5. Analytical model for mangrove friction

We will evaluate the mitigation effects of mangrove in reducing wave heights and velocities by both analytical and numerical solutions. We first derive an analytical formula to relate wave height reduction due to friction created by mangrove in the form $\eta = \eta_0 \exp(-\beta x)$, where x (m) is the distance traveled and β (m^{-1}) is a constant. Consider the linearized continuity and momentum Eqs. (8) and (9) involving the wave height η (m) and velocity u (m/s), given gravity g (9.81 m/s^2), water depth h (m) and friction coefficient γ (dimensionless). The friction term γ can be rewritten in the Manning form Eq. (10), with the Manning coefficient n ($sm^{-1/3}$). This may be further reduced to the linear approximation involving linear friction coefficient R_f (s^{-1}). Linearization is used to enable the derivation of analytical solution.

$$\frac{\partial\eta}{\partial t} = -h\frac{\partial u}{\partial x} \tag{8}$$
$$\frac{\partial u}{\partial t} = -g\frac{\partial\eta}{\partial x} - \frac{\gamma}{h}u|u| \tag{9}$$
$$-\frac{\gamma}{h}u|u| \approx -R_f u = -\frac{gn^2}{h^{4/3}}u|u| \tag{10}$$

The analytical solution for Eqs. (8)–(10) can be expressed in the form (Koh, 2004)

$$u = ae^{-\beta x}\sin(\sigma t - kx + \alpha),$$
$$\eta = abe^{-\beta x}\sin(\sigma t - kx).$$

We are interested in the decay factor β due to friction in the forms indicated below, where β (m^{-1}) is the decay number, indicating the rate of decay per m.

$$\eta \approx \eta_0 e^{-\beta x},\quad u \approx u_0 e^{-\beta x}$$

The linear friction coefficient R_f (s^{-1}) is related to dimensionless friction coefficient γ and Manning coefficient n and maximum velocity v_0 by the following relationships Eqs. (11) and (12), the details of which are available in Koh (1991). Further, the wave number k (m^{-1}) is given by Eq. (13), where σ (s^{-1}) is the wave frequency. The decay number β (m^{-1}) is given by Eq. (14).

$$R_f = \left(\frac{\gamma}{h}v_0\frac{2}{\pi}\right),\ \text{with } \gamma = \frac{gn^2}{h^{1/3}} \tag{11}$$
$$\text{Hence, } R_f = \left(\frac{gn^2}{h^{1/3}\cdot h}v_0\frac{2}{\pi}\right) = \frac{gn^2}{h^{4/3}}v_0\frac{2}{\pi} \tag{12}$$
$$\text{Further, } k^2 = \frac{\sigma^2}{gh}\left\{\frac{1}{2} + \frac{1}{2}\sqrt{1 + \frac{R_f^2}{\sigma^2}}\right\} \tag{13}$$
$$\text{and } \beta = \frac{R_f\sigma}{2ghk}m^{-1} \tag{14}$$

In a given study we assume that the following five values are known or can be computed: σ, n, h, g, v_0. Then we can calculate the following four values: γ, R_f, k, β. The value of β expressing the strength of friction to reduce wave heights can be estimated quite easily under two conditions: (a) $\left(\frac{R_f}{\sigma}\right) \ll 1$ and (b) $\left(\frac{R_f}{\sigma}\right) \gg 1$ as shown below.

Case (a)

If $\left(\frac{R_f}{\sigma}\right) \ll 1$, then

$$\frac{R_f^2}{\sigma^2} \approx 0$$

and $k = \frac{\sigma}{\sqrt{gh}}$.

Case (b)

If $\left(\frac{R_f}{\sigma}\right) \gg 1, \text{then}\left(\frac{R_f}{\sigma}\right) \gg 1$. Further,

$$k^2 = \frac{\sigma^2}{gh}\frac{R_f}{2\sigma} = \frac{\sigma R_f}{2gh}\text{or}k = \sqrt{\frac{\sigma R_f}{2gh}}$$

Then $\beta = \frac{R_f\sigma}{2ghk} = \frac{R_f\sigma}{2gh}\sqrt{\frac{2gh}{\sigma R_f}} = \sqrt{\frac{R_f\sigma}{2gh}} = k.$

$$\text{Finally, } \beta = \frac{n}{h}\sqrt{\frac{2v_0}{Th^{1/3}}}(m^{-}1), \tag{15}$$
$$\text{and } \hat{x} = -\frac{1}{\beta}\ell n(0.5)(m). \tag{16}$$

In the above $\hat{x}$ = half distance (m), T = wave period (s) and v_0 = wave maximum velocity (ms^{-1}). For friction over mangrove forests, condition (b) prevails. The decay number β depends on Manning coefficient n, water depth h, wave period T, and maximum particle velocity v_0. Given known values of these four parameters, the value of β (m^{-1}) can be calculated by Eq. (15), while the half distance $\hat{x}$ (m) (distance it takes the wave height to reduce by half) is calculated by Eq. (16). Further details regarding analytical solution in related field is available in Liu et al. (2003).

Table 1 provides the values of β ($\times 10^{-3}$ m^{-1}) as a function of four parameters: Manning coefficient n, wave period T, mean water depth h of 2 m, and incident velocity v_0 of 2.5 m/s. Table 2 provides the corresponding half distance $\hat{x}$ (m). For example, for a given value of n = 0.2 $sm^{-1/3}$ and T = 60 min, β is 2.97 $\times 10^{-3}$ m^{-1} and half distance $\hat{x}$ is 208.77 m. This means that it will need a mangrove width of 208.77 m to reduce wave height by half. To relate

Table 1
Decay number β (n,T) m^{-1} with v_0 = 2.5 m/s and h = 2 m.

T (minutes)	n ($sm^{-1/3}$)						
	0.1	0.2	0.3	0.4	0.5	0.6	0.7
10	3.64	7.27	10.91	14.55	18.19	21.82	25.46
20	2.57	5.14	7.72	10.29	12.86	15.43	18.00
30	2.10	4.20	6.30	8.40	10.50	12.60	14.70
40	1.82	3.64	5.46	7.27	9.09	10.91	12.73
50	1.63	3.25	4.88	6.51	8.13	9.76	11.39
60	1.48	2.97	4.45	5.94	7.42	8.91	10.39

Table 2
Half distance $\hat{x}$ (n,T) m with $v_0 = 2.5$ m/s and $h = 2$ m.

T (minutes)	n ($sm^{-1/3}$)						
	0.1	0.2	0.3	0.4	0.5	0.6	0.7
10	170.46	85.23	56.82	42.61	34.09	28.41	24.35
20	241.06	120.53	80.35	60.27	48.21	40.18	34.44
30	295.24	147.62	98.41	73.81	59.05	49.21	42.18
40	340.92	170.46	113.64	85.23	68.18	56.82	48.70
50	381.16	190.58	127.05	95.29	76.23	63.53	54.45
60	417.54	208.77	139.18	104.38	83.51	69.59	59.65

Manning coefficient n to mangrove characteristics, Eq. (17) may be useful. Various combinations of n, T, h and v_0 may be used to provide a preliminary assessment of the role of mangrove forests in reducing tsunami wave heights and velocities by means of the simplified analytical model Eqs. (15) and (16). However, we will also use the numerical model TUNA-RP to simulate the complex wave along the coastal seas in Penang in a later section for comparison.

6. Preliminary simulations

The existence of complicated wave structures is demonstrated by improving simulation resolutions with the use of smaller grid sizes $\Delta x = 40$, 20, 10, 5, 2.5 and 1.25 m. Fig. 6 illustrates the waves structures with various grid resolutions $\Delta x = 40$, 20, 10, 5, 2.5 and 1.25 m, clearly showing the wave structures at small grids of 2.5 m and 1.25 m. With grid size of 40 m and 20 m, the wave structures show no detailed features (Fig. 6a and Fig. 6b). But at $\Delta x = 10$ m, the waves show obvious fluctuations at locations between 5000 m and 9000 m (Fig. 6c). These fluctuations are not reduced

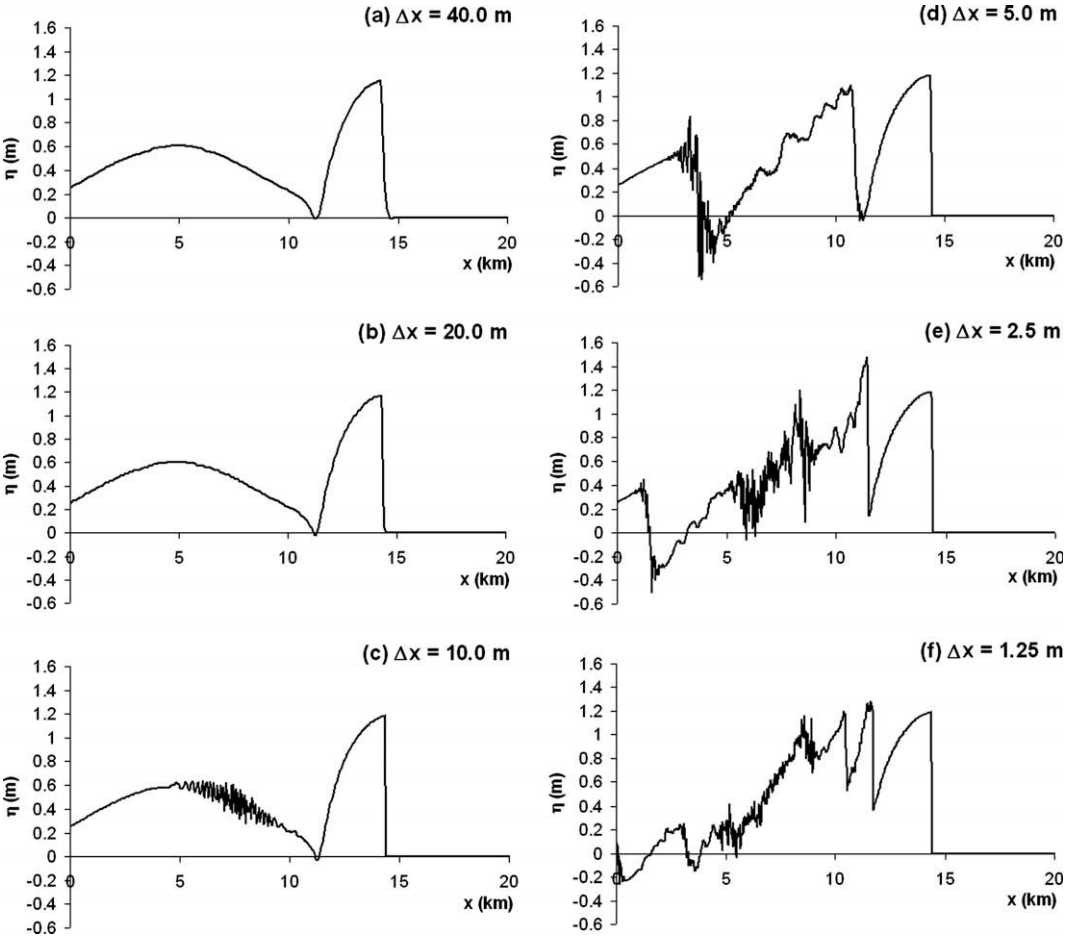

Fig. 6. Heights η at $t = 0.3$ h for every halving of grid size Δx, from 40 m to 1.25 m, $n = 0.0$.

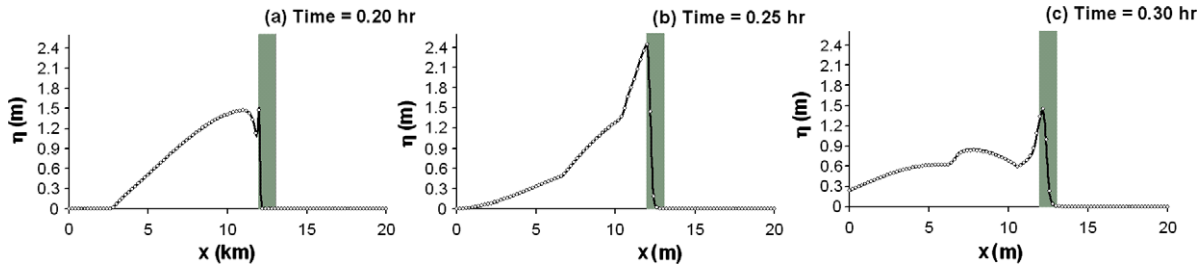

Fig. 7. Comparison between results using Manning friction term $n = 0.22$ (circle) and drag resistance term $C_D = 0.9$ (line) from 12 to 13 km.

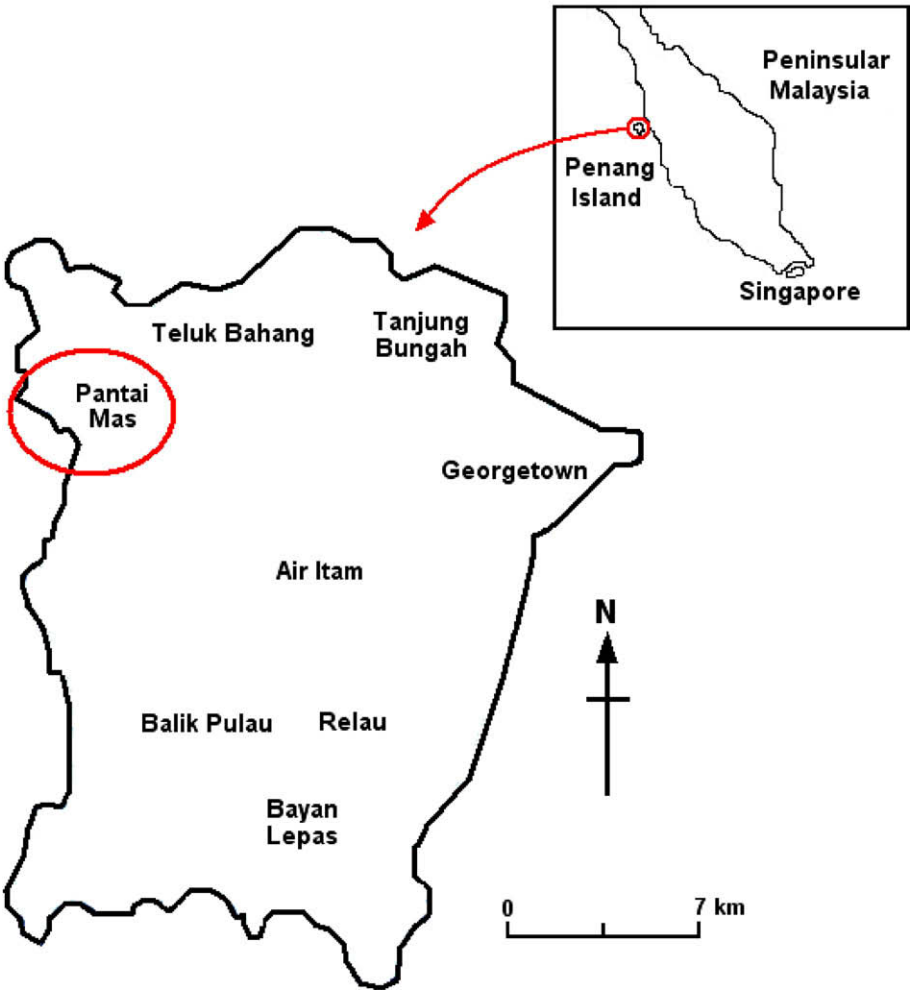

Fig. 8. Location of study site Pantai Mas in Penang Island.

by increasing frictions. Further at $\Delta x = 5$ m, 2.5 and 1.25 m, the numerical solutions are given in Fig. 6d, e and f. The reasons for these oscillations are not clear, hence further research is needed. From the analysis of further test results, it may be deduced that grid size of 40–50 m is adequate to resolve the overall runup wave heights, as reported in the literature. Hence, for the purpose of practical simulations to obtain maximum runup wave heights, grid sizes of about 40–50 m are adequate. In view of this observation, we will utilize grid size of 20–40 m for the purpose of assessing the role of mangroves in reducing runup wave heights subject to various scenarios.

We will now perform analysis of the impact of mangroves by means of drag and inertia coefficients represented by Eqs. (6) and (7) on wave heights and velocities. First we carefully check that TUNA-RP incorporating mangrove resistance in the form of Eq. (7) performs appropriately by comparing the simulations with those computed by means of equivalent Manning n as in Eq. (17), expressing the relationship between Manning coefficient n and drag coefficient C_d.

$$n = \sqrt{\frac{C_d A_0 D^{1/3}}{2g\Delta x\Delta y}} \tag{17}$$

The grid size Δx used in the test simulation is 20 m. The tsunami wave period T is 10 min and the incident offshore wave height H is 1 m. The presence of the mangrove forest in the model can be simulated using either the drag resistance term C_d in Eq. (7) or the Manning friction term n given in Eq. (10). In the case of drag resistance term, the internal computation of the drag coefficient is performed based upon the information of the mangrove forest given as input, based upon field survey results. In this test simulation, the following mangrove forest information is used, represent-

Fig. 9. *Avicennia officinalis* in Pantai Mas mangrove forest.

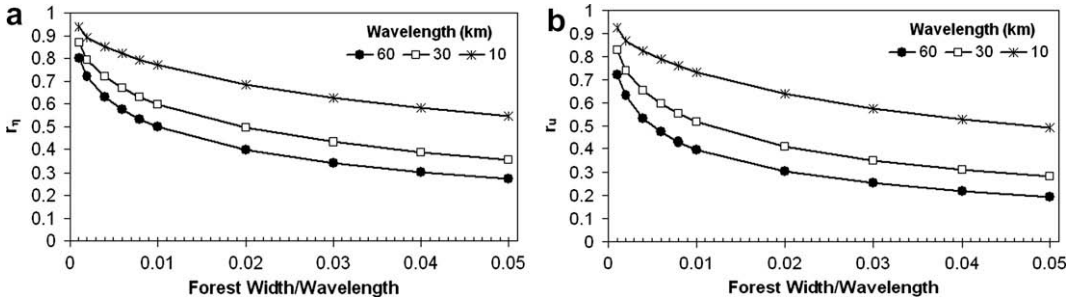

Fig. 10. Reduction ratios of elevation r_η (left) and velocity r_u (right) as a function of forest width relative to wavelength.

ing a typical mangrove reported in the literature (Mazda et al., 1997) and in Penang. Leaf porosity P_L is 0.03, number of trees per 100 m^2 N_T is 30 and number of roots per tree N_R is 100. Further diameter of stem D_T is 0.15 m, diameter of each root D_R is 0.035 m and diameter of leaf part D_L is 2 m. Finally height of root part H_R is 1 m, height of stem part H_T is 2 m, height of leaf part H_L is 8 m and forest width W is 1000 m. Fig. 7 shows close agreement (at three time steps) between the two simulation results, one using drag coefficient C_D and the other using Manning coefficient n, indicating proper performance of TUNA-RP incorporating mangrove resistance.

7. Simulation results

Measurements of the mangrove trees were conducted in the mangrove forest located at Pantai Mas, Penang (Fig. 8). Mangroves of the species *Avicennia officinalis* are observed to be abundant near the coasts (Fig. 9) but as we approach further inland, the species *Bruguiera cylindrica* can be found. The diameters of the trunks, roots, heights of the roots as well as number of trees and roots are measured in quadrants of 10 m by 10 m. Other parameters such as the heights of the tree trunks and canopy, diameters of the canopy and the porosity of the canopy are estimated. These measurements of the mangrove trees are then incorporated into the runup model TUNA-RP as described above to simulate the mitigation effect of mangrove forest. The following input parameters for *A. ofiicinalis* are used: P_L = 0.03; N_T = 20 trees per 100 m^2; N_R = 300 roots per tree; D_L = 3.0 m; D_T = 0.18 m; D_R = 0.008 m; H_L = 3.0 m; H_T = 5.5 m; H_R = 0.18 m.

The effects of mangrove are measured by the reduction ratio as defined below,

$$r_\eta = \frac{\eta_{\text{formax}}}{\eta_{\max}}; r_u = \frac{u_{\text{formax}}}{u_{\max}}$$

In the above r_η = reduction ratio of elevation, $_{\text{formax}}$ = maximum elevation with mangrove forest and $_{\max}$ = maximum elevation without mangrove forest. Further r_u = reduction ratio of velocity; u_{formax} = maximum velocity with mangrove forest; $u_{\max}$ = maximum velocity without mangrove forest.

Fig. 10a shows the reduction ratios of elevation r_η as a function of dimensionless parameter defined as forest width/wavelength for a range of wavelengths. Similarly, Fig. 10b shows the reduction ratios of velocity r_u. It should be noted that the maximum values, η_{formax}, $\eta_{\max}$, u_{formax} and $u_{\max}$ are measured at locations behind the mangrove forest. For example, let us consider a wavelength of 10 km. If the maximum wave height and velocity at the shore without a mangrove forest is 1.0 m and 1.0 m/s, respectively, then in the presence of a mangrove forest of 100 m width (or 1% of wavelength of 10 km), the maximum wave height and velocity will be reduced to 0.78 m and 0.73 m/s, respectively. Similarly in the presence of the mangrove forest of 500 m width (or 5% of wavelength of 10 km), the maximum wave height and velocity will be reduced to 0.55 m and 0.50 m/s, respectively. The reduction ratios vary significantly depending on the forest widths and the wavelengths as well as the mangrove characteristics. Larger widths of forest relative to the wavelength tend to have lower (better) reduction ratios for given wave elevation and velocity.

8. Conclusion

We implement an improved radiation open boundary condition to allow waves to radiate out of the computational domain without reflections by means of a 4-point interpolation technique in conjunction with the method of characteristics. The effects of mangrove forest in reducing tsunami wave heights and velocities are then simulated by the incorporation of the Morison Equation to represent friction provided by mangrove forest along the coasts of Penang. Analytical and numerical results are found to agree well in general. The reduction ratios in wave heights and velocities vary significantly depending on several factors such as wave heights, wave period and wavelength as well as mangrove characteristics including forest widths and density. For a wave of 10 km wavelength, with wave height and velocity of 1.0 m and 1.0 m/s, respectively at the shore without a mangrove forest, then a mangrove forest of 500 m width (or 5% of wavelength of 10 km) may provide a reduction ratios for wave height and wave velocity of about 0.55 and 0.50, respectively.

Acknowledgement

Financial support provided by Grants #305/PMATHS/613131, #1001/PPTM/817006 and #1001/PMATHS/817025 is gratefully acknowledged.

References

Baird, A.H., 2006. Myth of green belts. Viewpoint, SAMUDRA Report No. 44.
Chatenoux, B. and Peduzzi, P., 2006. Analysis of the Role of Bathymetry and Other Environmental Parameters in the Impacts from the 2004 Indian Ocean Tsunami. UNEP/DEWA/GRID-Europe, Switzerland.
Harada, K. and Imamura, F., 2000. Experimental study on the resistance by mangrove under the unsteady flow. In: Proceeding of the 1st Congress of APACE pp. 975–984.
Harada, K. and Imamura, F., 2003. Evaluation of tsunami reduction by control forest and possibility of its use for mitigation. In: Proceedings of Coastal Engineering, Japan Society of Civil Engineers, pp. 341–345. (In Japanese).
Harada, K., Imamura, F., 2005. Effects of coastal forest on tsunami hazard mitigation – a preliminary approach investigation. Adv. Nat. Technol. Haz. Res. 23, 279–292.
Harada, K. and Kawata, Y., 2004. Study on the effect of coastal forest to tsunami reduction. Annuals of Disas. Prev. Res. Inst., Kyoto Univ., No. 47 C.
Hiraishi, T., Harada, K., 2003. Greenbelt tsunami prevention in south-Pacific region. Report of the Port and Airport Research Institute 42 (2), 3–25.
Koh, H.L., 1991. Modeling tidal dynamics in western channel: some theoretical considerations. J. Fiz. Mal. 12, 43–48.
Koh, H.L., 2004. Environmental and Ecosystem Modeling (Pemodelan Alam Sekitar dan Ekosistem), Universiti Sains Malaysia Publishers, p. 379.

Koh, H.L., Teh, S.Y., Liu, P.L.-F., Md. Ismail, A.I. and Lee, H.L., 2008a. Simulation of Andaman 2004 tsunami for assessing impact to Malaysia. J. Asian Earth Sci. in press.

Koh, H.L., Teh, S.Y., Md. Ismail, A.I., Lee, H.L. and Kew, L.M., 2008b. Simulation of Andaman tsunami for northwest Malaysia. In: Teruyuki Kato (Ed.), Proceedings of the International Symposium on the Restoration Program from Giant Earthquakes and Tsunamis, 22–24 January 2008, University of Tokyo, Phuket, Thailand, pp. 313–318.

Liu, P.L.-F., Lynett, P., Synolakis, C.E., 2003. Analytical solutions for forced long waves on a sloping beach. J. Fluid Mech. 478, 101–109.

Marchuk, A.G. and Anisimov, A.A., 2001. A method for numerical modeling of tsunami run-up on the coast of an arbitrary profile. In: Proceedings of International Tsunami Symposium (ITS), 7-10 August 2001, Washington, USA, pp. 933–940.

Mazda, Y., Kanazawa, N., Wolanski, E., 1995. Tidal asymmetry in mangrove creeks. Hydrobiologia 295, 51–58.

Mazda, Y., Wolanski, E., King, B., Sase, A., Ohtsuka, D., Magi, M., 1997. Drag force due to vegetation in mangrove swamps. Mangroves and Salt Marshes 1, 193–199.

Shuto, N., 1987. The effectiveness and limit of tsunami control forests. Coastal Eng in Japan 30, 143–153.

Teh, S.Y., 2008. Tsunami Impact Modeling of Coastal Regions and Vegetation Recovery. PhD Thesis, Universiti Sains Malaysia.

Teh, S.Y., Koh, H.L., Izani, A.M.I. and Lee, H.L., 2008. Modeling tsunami runup by moving boundary. In: Teruyuki Kato (Ed.), Proceedings of the International Symposium on the Restoration Program from Giant Earthquakes and Tsunamis, 22-24 January 2008, University of Tokyo, Phuket, Thailand, pp. 301–306.